

# COSMOLOGY WITH SUPERNOVAE 1A

Smadja Gérard

*IPNL, Université Cl. Bernard Lyon 1*

*F69622 Villeurbanne Cedex*

*g.smadja@ipnl.in2p3.fr*

**Abstract** The basic relations between the luminosity distance, the matter density  $\Omega_M$ , and the cosmological constant  $\Omega_\Lambda$  are derived. The universal character of the luminosity of SN1a is described, and the experimental status of the determinations of the Hubble constant,  $\Omega_M$ , and  $\Omega_\Lambda$  are recalled. The large supernovae surveys foreseen in the near future, and their expected performances are reviewed. Some aspects of the supernovae explosions are briefly summarised

**Keywords:** Supernovae, Friedmann's equation, luminosity distance, Hubble expansion, cosmological constant, matter density, dust, evolution

## Introduction

We shall assume that the mean luminosity of Type Ia supernovae does not change with redshift: they are standard. There is no indication at present for any such variation, although the bounds are weak. Should future data contradict this assumption at some level, the present values of the densities  $\Omega_M, \Omega_\Lambda$  should be appropriately corrected, but the analysis discussed here would not be drastically altered.

The observed luminosity of supernovae is in this context a direct indicator of their distance (using a modified inverse squared law), and the redshift of the host galaxy lines gives its recession velocity. The relation between distance and redshift reflects the history of the Hubble 'constant' between the time of emission of the SN light and its observation today. In a homogeneous and isotropic universe, this variation with time (or redshift) can be explicitly obtained from the Friedman equation which we shall recall. Since the first quantitative results were published

by [6] and [7], the indications for a finite cosmological constant have been strengthening.

## 1. Distances in curved space

### 1.1 2D Geometry

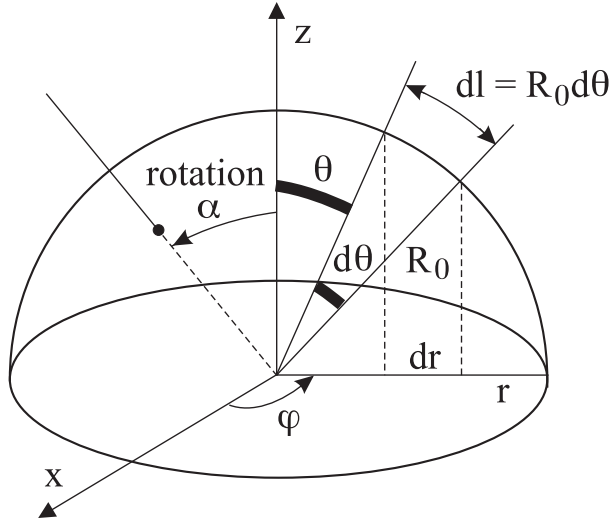


Figure 1. Distances on the 2D surface of a sphere

The 2D surface of a sphere of radius  $R_0$  gives an intuitive introduction to the relation between the projected coordinates  $(r, \phi)$  and distances. The geodesic line element is

$$dl = \frac{dr}{\sin \theta} = \frac{dr}{\sqrt{1 - r^2/R_0^2}}$$

The translation operation does not preserve the surface, and must be replaced by a rotation. This will be directly transposed to the 3D surface of a 4D sphere, which might describe the universe at large scales (if curved).

### 1.2 3D curved space : changing the origin

The homogeneity of space at large scales imposes a constant radius.

$$x_1^2 + x_2^2 + x_3^2 + kx_4^2 = kR_0^2$$

with  $k = -1, 0, 1$  depending on the sign of the curvature (the constant  $R_0$  is related to but not equal to the 3D curvature). Let us stress that the auxiliary 4th coordinate is NOT time. A change of origin cannot be described by a translation, but rather by 3D or 4D 'rotations' which leave the line element

$$dl^2 = dx_1^2 + dx_2^2 + dx_3^2 + kdx_4^2 \quad (1.1)$$

invariant. The usual spherical coordinates can be introduced if  $k > 0$ .

$$\begin{aligned} x_1 &= R_0 \sin \chi \sin \theta \cos \phi \\ x_2 &= R_0 \sin \chi \sin \theta \sin \phi \\ x_3 &= R_0 \sin \chi \cos \theta \\ x_4 &= R_0 \cos \chi \end{aligned}$$

The line element can be expressed as

$$dl^2 = a(t)^2 R_0^2 \left[ r_a (d\theta^2 + \sin^2 \theta (d\phi)^2) + \frac{(dr_a)^2}{1 - kr_a^2} \right] \quad (1.2)$$

with

$$r_a = \frac{r}{R_0} = \sin \chi \quad (1.3)$$

The scale factor  $a(t)R_0$  converts (comoving) dimensionless coordinates to distances at time  $t$ . A change of origin should be described by a rotation involving the 4th auxiliary coordinate. Assume  $k = 1$

$$\begin{aligned} x_4^* &= x_4 \cos \chi + x_3 \sin \chi = R_0 \cos \chi^* \\ x_3^* &= x_3 \cos \chi - x_4 \sin \chi = R_0 \sin \chi^* \cos \theta^* \\ x_2^* &= x_2 = \sin \chi^* \sin \theta^* = \sin \chi \sin \theta \end{aligned}$$

If  $k = -1$  hyperbolic lines should be substituted with  $\cos \rightarrow \cosh$ ,  $\sin \rightarrow \sinh$ , and no minus sign in the formulae. The observed angle of a distant object is obtained from

$$\theta^* = \pi/2, \quad \sin \theta = R_0 \sin \chi^* / R_0 \sin \chi$$

and by analogy with the usual relation, an angular distance is defined as  $\sin \theta = L_A/d_A$ , where  $L_A = a(t_e)R_0 \sin \chi^*$  is the diameter of the object (galaxy) at time  $t = t_e$ , the emission time, and  $d_A = a(t_e)R_0 \sin \chi$ , its angular distance.

## 2. Luminosity and distance

### 2.1 The energy flux

We have already introduced the spherical coordinate transformations associated with a change of origin. The telescope has a diameter  $D_0 = a(t_0)r^* = a(t_0)R_0 \sin \chi^*$  with a local origin on the earth, and its area is  $\Delta S = \pi D^2/4$ . The scale factor  $a(t_0)$  is the universal scale at the time of observation  $t_0$ , today (in contrast with the case of the angular distance), and is usually set to 1.

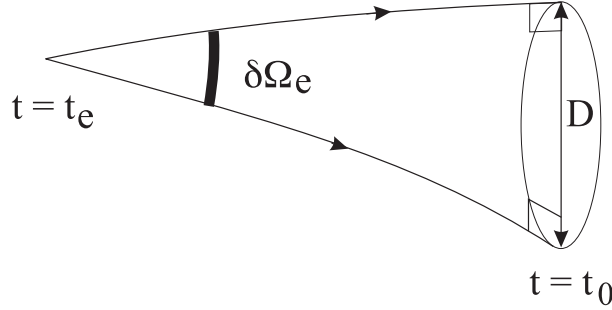


Figure 2. Solid angle at emission and Telescope diameter

The number of photons is conserved from emission to observation:

$$\frac{dN_\gamma}{dt_0 dS} dt_0 \Delta S = \frac{dN_\gamma}{dt_e d\Omega_e} dt_e \left( \frac{\Delta S}{4\pi a^2(t_0) r^2(z_e)} \right)$$

The flux is reduced by two factors equal to  $(1+z)^{-1}$ : the time dilatation  $dt_e/dt_0$  and the redshift  $a(t_0)/a(t_e)$ .

$$\frac{dW_0}{dt_0 dS} dt_0 \Delta S = \frac{1}{(1+z)^2} \frac{dW_e}{dt_e d\Omega_e} dt_e \left( \frac{\Delta S}{4\pi a^2(t_0) r^2(z_e)} \right)$$

Defining the (rest frame) luminosity  $L$  as

$$L = \frac{dW_e}{dt_e d\Omega_e}$$

$$\frac{dW_0}{dt_0 dS} \Delta S = L \frac{\Delta S}{4\pi d_L^2} \quad (2.1)$$

with

$$d_L = a(t_0)(1+z_e)r(z_e) = (1+z_e)r(z_e) \quad (2.2)$$

the luminosity distance, while  $r(z_e) = R_0 \sin \chi_e$ , the (comoving) coordinate at redshift  $z_e$ .

## 2.2 From redshift to distance

It is seen in figure 3 that along the ray trajectory,

$$dl = cdt = a(t) \frac{R_0 dr_a}{\sqrt{1 - k(r_a)^2}} = R_0 a(t) d\chi$$

(the variable  $r_a = r/R_0$  is the same as in equation (1.3) of subsection 1.2). One obtains

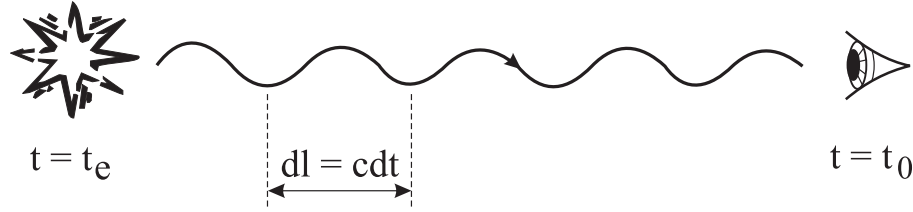


Figure 3. Propagation of a light ray from the SNIa to an observer

$$R_0 d\chi = \frac{cdt}{a(t)} = c \frac{da}{a(da/dt)}$$

$$R_0 \chi = c \int_{a(t_e)}^{a(t_0)} \frac{da}{a(da/dt)} = c \int_{a(t_e)}^{a(t_0)} \frac{da}{a^2(da/dt)}$$

The ratio  $\dot{a}/a = H(z)$  is the Hubble 'constant' at redshift  $z$ , and we can switch from the scale variable  $a(t)$  to the redshift  $z$  with the relation

$$a(z) = \frac{a_0}{1+z} = \frac{a(z=0)}{1+z} \quad \text{the Doppler formula}$$

so that  $dz = -da/a^2$ .

The final result is

$$R_0 \chi_e = c \int_{z_0}^{z_e} \frac{dz}{H(z)} \quad (2.3)$$

The function  $H(z)$  has been derived from Friedmann's equation in the lecture of professor D. Langlois:

$$H(z)^2 = H_0^2 \left( \Omega_M(z) + \Omega_R(z) + \Omega_\Lambda + \frac{\Omega_k}{a(z)^2} \right) = H_0^2 h^2(z)$$

with  $\Omega_k = 1 - \Omega_M(z=0) - \Omega_R(z=0) - \Omega_\Lambda$ . The reduced energy densities are known functions of the redshift  $z$ ,  $\Omega_i(z) = \Omega_i(0)(1+z)^{3(1+w_i)}$  where

$w_i$  is the ratio between the partial pressure  $p_i$  and the energy density  $\rho_i$  ( $w_1 = 0$  for the non relativistic matter,  $w_2 = 1/3$  for neutrinos and photons, and  $w_3 = -1$  for the cosmological constant). The luminosity distance  $d_L$  is obtained from equations (1.3),(2.1),(2.2) with different expressions according to the value of  $k$ .

$$\begin{aligned} d_L &= (1 + z_e)r(z_e) = (1 + z_e)R_0 \sin \chi_e & k = 1 \\ d_L &= (1 + z_e)r(z_e) = (1 + z_e)R_0 \sinh \chi_e & k = -1 \\ d_L &= (1 + z_e)r(z_e) = (1 + z_e)R_0 \chi_e & k = 0 \end{aligned}$$

- $d_L$  is a function of the history of the expansion rate ('Hubble constant') along the ray trajectory.
- $a(z = 0) = 1$  has been assumed, else,  $a(0)R_0$  should be substituted to  $R_0$  in the previous equations.
- if  $k > 0$  there is a maximal distance  $a(0)R_0$  in the universe (it does not seem to be the case).

One can define a function  $\sinh \chi$ , with values equal respectively to  $\sin \chi$ ,  $\sinh \chi$ ,  $\chi$ , depending on the value of the curvature coefficient  $k = 1, -1, 0$ .

The spherical (or hyperbolic) coordinate  $\chi$  is evaluated from the integral

$$I(z_e) = \frac{c}{a_0 H_0} \int_{z_0}^{z_e} \frac{dz}{h(z)} \quad (2.4)$$

The comoving coordinate  $r(z_e)$  can then be expressed as a function of  $I(z)$ :

$$r(z_e) = R_0 \sinh \left( \frac{I(z_e)}{a_0 R_0 H_0} \right) \quad (2.5)$$

$$d_L(z_e) = (1 + z_e)r(z_e) \quad (2.6)$$

The integral  $I(z)$  is a function of the parameters  $\Omega_M$ ,  $\Omega_R$ ,  $\Omega_\Lambda$  via the Friedman equation. The radiation density is however negligible in the present universe, as supernovae can only be observed (and produced!) only up to  $z \sim 2$ . The variation of the luminosity of SNIae as a function of the redshift  $z$  is then directly and simply related to the energy density and the geometry of the universe on cosmological scales.

### 3. The Experimental method

#### 3.1 The Search for Supernovae

Supernovae are found by comparing observed telescope fields with reference fields. After correcting for the variation of the optical properties of the atmosphere (the seeing, which varies between 0.4" and 1.2" depending on the site and the date), a subtraction allows to select variable objects, such as supernovae, cepheids, quasars, Active Galactic Nuclei. An example is given in figure 7. The light curve and the spectral properties contribute to the identification. The first generation of surveys accumulated typically 200 supernovae over a period of five years, spread on a wide variety of instruments. A large angular domain is clearly the key to an efficient discovery rate at moderate values of  $z$ . Below  $z = 0.8$ , a few supernovae can be found each night in a field of a few square degrees.

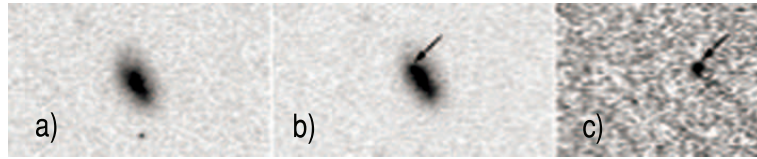


Figure 4. The detection of SNIae by subtraction from [1]

#### 3.2 Luminosity dispersion of SNIae and the time scale

The explosion leading to SNIae is characterised by a fixed mass scale, the Chandrasekhar mass, of about 1.4 solar mass, and the typical time scales in the SN rest frame are about 15 days for the rise time, and 20 days for the decline. Thanks to a scaling law to be explained later between the luminosity and the time evolution of supernovae, this spread can be impressively reduced when the light curve of the supernova is taken into account. The time scale for the light curve can be parametrised either by  $\Delta M_{15}$ , the drop in the measured (blue filter) magnitude between the peak, and its value 15 days after maximum, or by the stretch parameter  $s$ , defined by the ratio of time scales between the observed light curve shape and a reference template. A correction is then applied to the observed magnitude:

$$m_B = m_{obs} + 0.6(s - 1)$$

It is seen in figure 5 that the luminosity dispersion is reduced to 20 % once the stretch (or  $\Delta M_{15}$ ) corrections have been applied. This can be understood semi-quantitatively if the peak luminosity is directly correlated to the mass of  $^{56}\text{Ni}$  produced in the explosion. According to [8],[9] the opacity of the final  $^{56}\text{Ni}$  increases the diffusion time of the photons, and shifts the peak date to later values. It is quite remarkable that as stressed in [10], the luminosity and the stretch factor are also strongly correlated to spectral features such as the ratios of neighbouring pairs of Si and Ca lines in figure 6.

### 3.3 The Colour correction

It is apparent in figure 7 from [2] that there is a relation between the colour of the SN, as defined by the magnitude difference between two filters (B-V) or (V-I) at maximum, and the time-scale parameter  $\Delta M_{15}$ , which measures the luminosity. Most of this correlation is usually attributed to the galactic extinction in the host galaxy and in ours, without a compelling case. A significant part may be an intrinsic luminosity-colour correlation. The extinction correction does reduce the dispersion of SN luminosities. In addition, were it not applied, systematic effects from different extinctions in nearby and distant SNIae might arise.

## 4. The cosmological parameters

### 4.1 The determination of the Hubble constant

The determination of the Hubble constant from the luminosity of Type Ia supernovae requires the knowledge of their absolute magnitude. The distance of the host galaxy must then be measured directly without using its redshift. The standard tools are Cepheids, surface brightness fluctuations, or the Tully-Fisher relation for the rotation. This restricts the distance of the galaxy to our neighbourhood, and the statistics of supernovae in these galaxies is still quite small today. A recent review of the Cepheid calibration of the peak brightness can be found in [3],[4], where the absolute blue magnitude of SNIae is averaged from a sample of 9 supernovae to be  $M_B = -19.35 \pm 0.24$  after application of the time scale( $\Delta M_{15}$ ) and extinction corrections. Assuming this fixed luminosity, the value of the Hubble constant is then derived from the apparent magnitudes in a larger sample with  $z < 0.2$  to be  $H_0(t_0) = 59.7 \pm 6.3$  km/s/Mpc. It is indeed found in [11] that the dispersion around the  $1/z^2$  straight line (for  $z < 0.1$ ) is reduced to about 13 % after the time scale and colour corrections. Although the supernovae can be observed at larger distances than Cepheids, and have a smaller luminosity dispersion,



the benefit they give in the  $H_0$  determination is still dependent today on the knowledge of the distances of a very small sample of SN Ia.

## 4.2 Dust and evolution

The observed supernovae are less luminous than they would be in an empty universe with  $\Omega_\Lambda = \Omega_M = 0$ , and by an amount of 30 to 40%. Some unknown galactic or intergalactic dust might generate a similar attenuation. Although the present data do not rule out this contribution, the origin and nature of such a dust would need explanations. The present data in figure 8 of [12] hints that the  $z$  dependence might be turning around at  $z > 1$ , as predicted by cosmology, while the dust interpretation would favour an ever stronger decrease of the luminosity at large  $z$ , as seen in figure 9.

## 4.3 The matter and energy densities

Once the SNIae have been 'standardized' by the time scale and colour correction, a fit of the luminosities as a function of redshift, using equations (2.1) and (2.5) allows the determination of the parameters  $\Omega_M$  and  $\Omega_\Lambda$ . A large lever arm in  $z$  is needed, and the experiments combine different surveys, with different systematics. The probability contours found by the combination of the data sets available in 2003 are shown in figures 10 and 11 from [12], which includes 200 Supernovae:  $\Omega_M = 0.60 \pm 0.55$ ,  $\Omega_\Lambda = 1.3 \pm 0.7$ , and an  $w = -1.1 \pm 0.3$ . This result is compatible (to within 1 standard deviation) with the critical density measured by the 3K radiation (see the lecture of G. Smoot), with  $\Omega_M + \Omega_\Lambda = 1$  (flatness).

When the constraint of flatness is included, the contours are modified as indicated in the small ellipse in figure 10 and 11: the corresponding values are  $\Omega_M = 0.27 \pm 0.05$ , and  $\Omega_\Lambda = 0.73 \pm 0.22$

The remaining uncertainty concerns a possible evolution of supernovae from early times ( $z = 1$ ) to the present era. There are neither indications for such an evolution, nor strong limits. It is hoped that the future experiments, with large statistics at low and high  $z$ , and good spectroscopy will give quantitative estimates.

## 5. Future programmes

### 5.1 Short term

Up to now, the two main surveys by the HZT and SCP collaborations have been painstakingly gathered over a wide set of telescopes, distributed all over the world (WHT, VLT, CFHT, Keck, etc...in the US), with scarce but high quality data from HST. The detection beyond

$z = 0.3$  up to  $z = 1$  can be performed with instruments of 4m diameter (CFHT, WHT), while the spectral analysis needed for redshifts and classification requires typically (for  $z > 0.5$ ) a whole night on an 8m telescope (VLT, Keck).

Several dedicated surveys have now been initiated, the SNLS (Supernovae Legacy Survey) at CFHT and the GOODS ([13]) (Great Observatories Origin Deep Surveys) combining several large space instruments (Chandra, XMM, SIRTf, Hubble). The SNLS survey should provide over 5 years 700 SNIae with  $z > 0.3$ . It is shown in figure 12 how the SNLS survey, combined with a nearby supernovae sample obtained by SNIFS (Supernovae Integral Field Spectrometer) will reduce the statistical errors on  $(\Omega_M, \Omega_\Lambda)$  to  $(\pm 0.06, \pm 0.02)$  [14].

As has been discussed in the lecture of D. Langlois, the cosmological constant is only an approximate description of a scalar field with an equation of state  $p = w/\rho$ , where  $w \sim -1$ . All inflation models predict a variable ratio  $p/\rho$  as a function of  $z$  for this universal fluid, and the measurement of  $w$  and its variation would bring a crucial constraint to the elucidation of the properties of the field. A true fixed value of  $w = -1$  has been assumed in figure 13, and the error is seen to be  $\pm 0.1$ , decreasing to 0.03 if  $\Omega_M$  is determined from other experiments to an accuracy of 0.03.

The slope parameter  $w_1$  with  $w(z) = w_0 + zw_1$  will remain however very poorly known from the combination of the nearby (SNIFS) and distant (CFHT-LS) samples: space projects are needed to control the systematical errors to the accuracy needed.

## 5.2 Long term space projects

The ground observations are subject to large atmospheric corrections, which differ intrinsically in the blue (nearby SN) and the IR ranges (remote SN). They will unavoidably limit the quality of high statistics samples collected from the ground, and a dedicated effort for a large sample of SN collected in space is justified.

The Supernova Acceleration Probe (SNAP) has received support from NASA and DOE in the frame of the Joint Dark Energy Mission (JDEM), to be launched within the next ten years. The satellite proposed would be equipped with a 2m telescope. The focal plane consists of  $500 \times 10^6$  pixels, covering a field of view of about 1 square degree. It would give the instrument an outstanding capability to study:

- supernovae up to  $z = 1.7$
- weak lensing

- galactic evolution and clusters

The probability contours for  $\Omega_M$ ,  $\Omega_\Lambda$  as known today are shown in figure 14, and can be compared with the the design accuracy reached by the SNAP/JDEM project in figure 15. Extreme care is needed to provide a significant step in the accuracy on the parameter  $w$  and its variation with  $z$ , as all calibrations should reach or exceed the 1% accuracy level. On the other hand, the only other technique with a sensitivity to the equation of state parameter  $w$  is the measurement weak lensing, which is also at the edge of experimental analysis.

## 6. Acknowledgments

We would like to thank the physicists of the Supernovae Cosmology Project and the High Z Team, who have strongly stimulated the interest into the Supernovae studies worldwide. The french groups are particularly indebted to the SCP collaboration. Ed Baron has straightened several misconceptions concerning the explosion of SNIa. Most of this work was initiated thanks to an invitation of Svetlana Ivanovna, at the university of Dubna (Russia).

## References

- [1] D. Hardin et al., "Type Ia supernovae rate at  $z \sim 0.1$ " *Astronomy and Astrophysics* **362** (2000) 419
- [2] M. M. Phillips et al., "The reddening-free decline rate versus luminosity relationship for Type 1A Supernovae" *Astrophysical Journal* **118**(1999) 1766
- [3] A. Saha et al., "Cepheid calibration of the peak brightness of SNIa" *Astrophysical Journal* **551**(2001) 973
- [4] G. A. Tammann et al., "Cepheids, Supernovae,  $H_0$ , and the age of the universe" *A New Era in Cosmology Conference* (2001) (ASP Proceedings)
- [5] S. Perlmutter et al., "Measurements of the Cosmological Parameters  $\Omega$  and  $\Lambda$  from the first 7 Supernovae at  $z > 0.35$ " *Astrophysical Journal* **476** (1977) L63
- [6] S. Perlmutter et al., "Measurement of  $\Omega$  and  $\Lambda$  from 42 high red-shift supernovae", *Astrophysical Journal* **517**(1999) 1
- [7] A.G. Riess et al., "Observational evidence from Supernovae for an accelerating universe and a cosmological constant" *Astronomical Journal* **116**(1998)1009
- [8] D. Arnett, "Universality in SNIae and the Phillips Relation", *astro-ph/9908169*
- [9] D. Arnett, *Astrophysical Journal* **253** (1982) 785
- [10] P. Nugent et al., "Evidence for a spectroscopic sequence among type 1a supernovae", *Astrophysical Journal* **455** (1995) L147
- [11] M. M. Phillips et al. "The reddening free decline rate versus luminosity relationship for Type 1a Supernovae" *Astrophysical Journal* **118**(1999)1766

- [12] J. Tonry et al. "Cosmological results from High-z Supernovae" *Astrophysical Journal* **594**(2003)1
- [13] <http://www.stsci.edu ftp/science/goods>
- [14] <http://supernovae.in2p3.fr/astier/loi.ps>
- [15] <http://snap.lbl.gov> (SNAP Science, Mission, and Simulation, presentation by A. Kim)
- [16] D. N. Spergel et al. (WMAP), "First Year of WMAP observations, determination of the cosmological parameters" astro-ph/0302209 (June 2003), accepted in *Astrophysical Journal*
- [17] S. W. Allen et al. , *Monthly Notices of the Royal Astronomical Society* **342** (2003)287
- [18] R. A. Knop et al., "New Constraints on  $\Omega_M$ ,  $\Omega_\Lambda$ , and  $w$  from an independent set of eleven high-redshift supernovae observed with HST" astro-ph/0309368 accepted in *Astrophysical Journal*

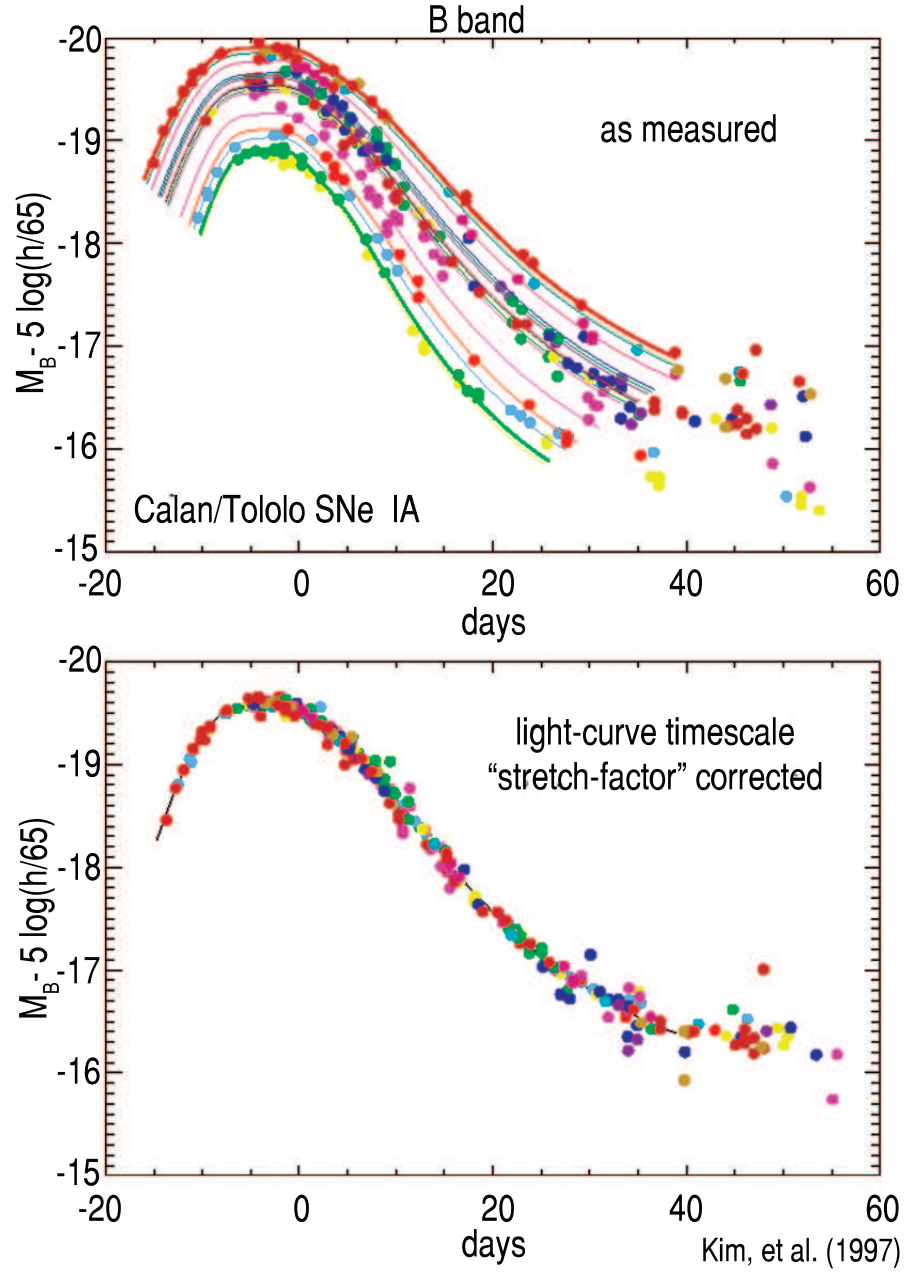
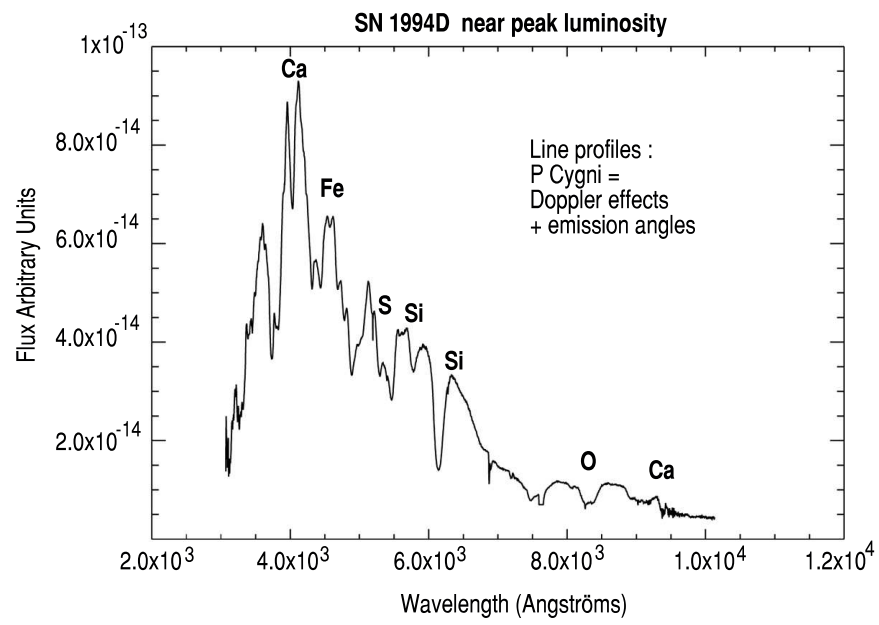


Figure 5. Distribution of the peak luminosity without and with stretch correction



*Figure 6.* The main features of the SNIa spectrum

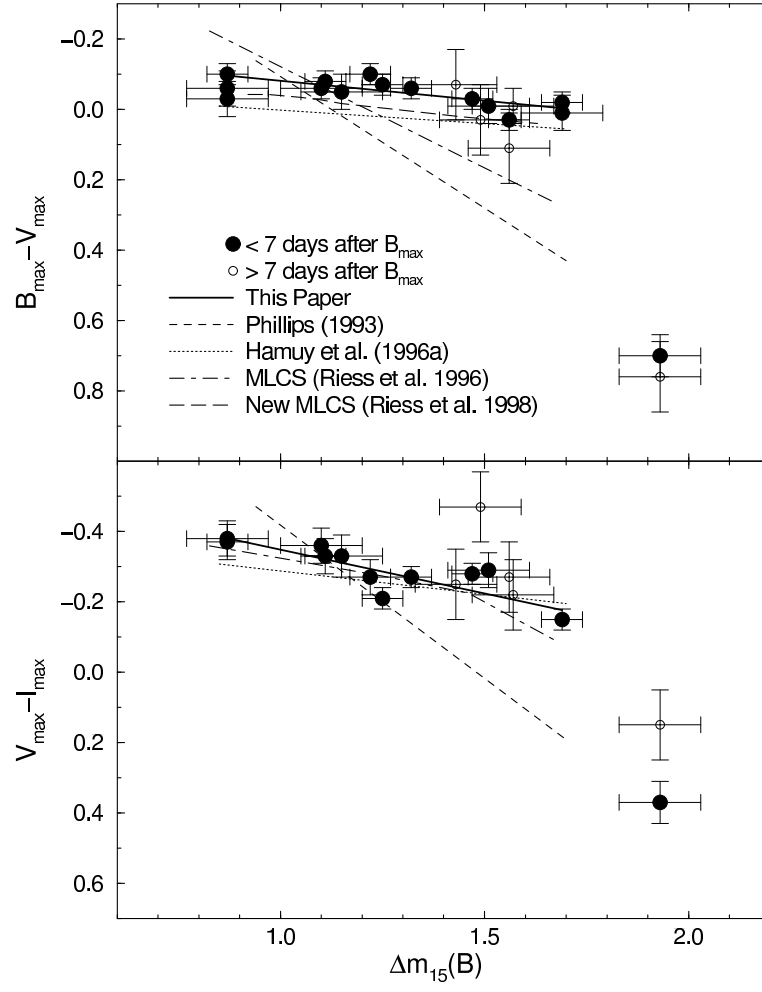


Figure 7. The correlation between colour and  $\Delta M_{15}$

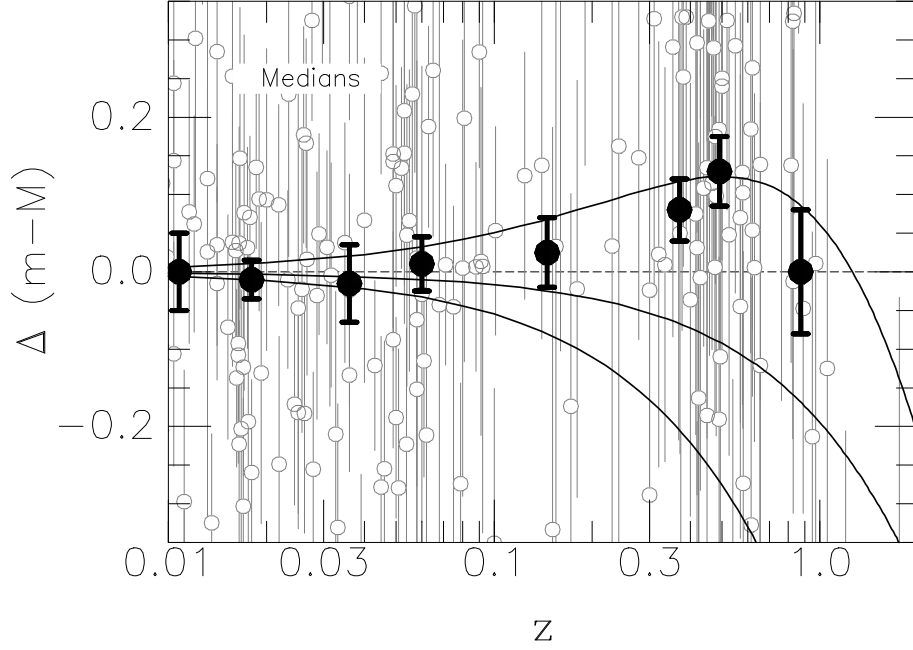


Figure 8. Comparison with an empty universe (from [12])

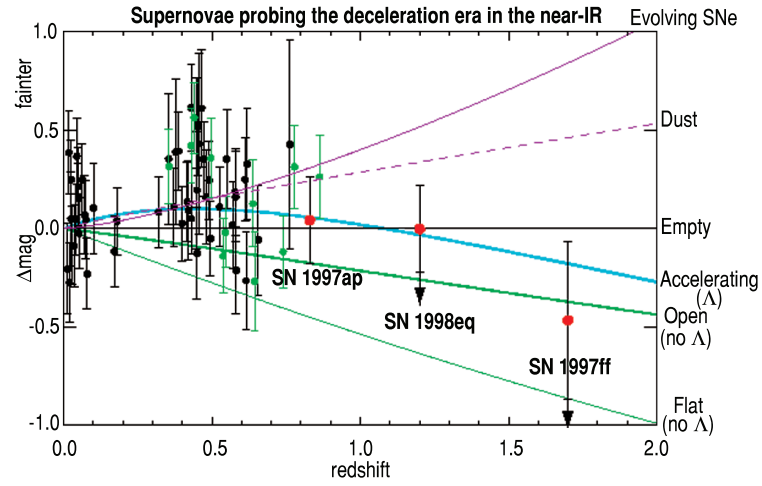


Figure 9. Comparison of different models with a flat (empty) universe



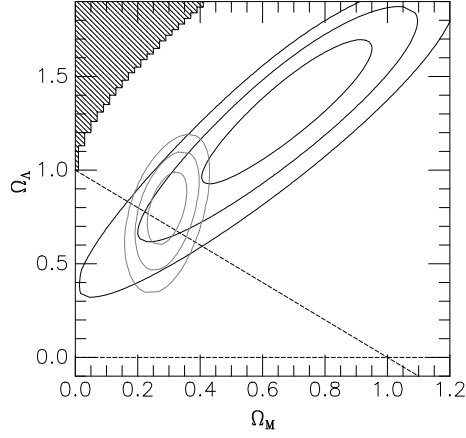


Figure 10. Contour plots for  $\Omega_\Lambda$  and  $\Omega_M$

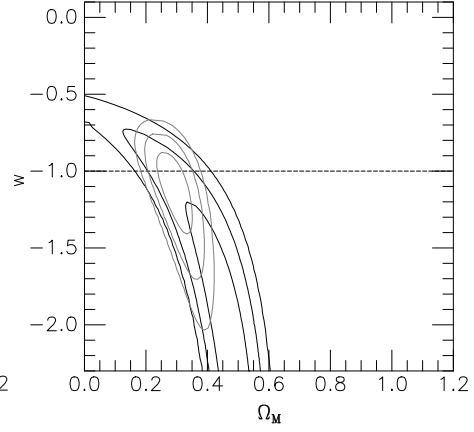


Figure 11. Contour plots for  $\Omega_\Lambda$  and  $w$

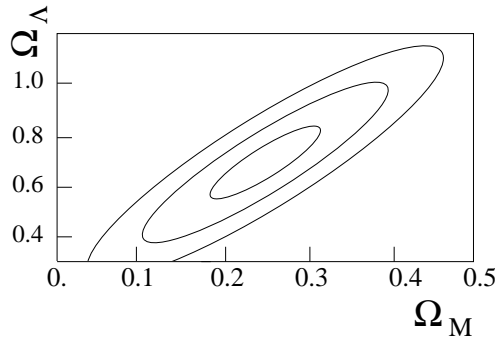


Figure 12. CFHLS contours for  $\Omega_M, \Omega_\Lambda$

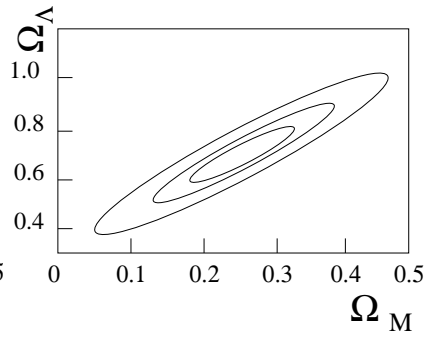


Figure 13. Combining SNLS(distant) and SNIFS(nearby) Supernovae

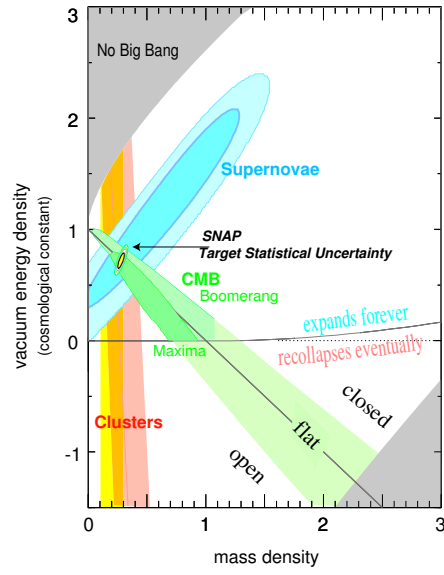


Figure 14. SNAP contours for  $\Omega_M, \Omega_\Lambda$  from [15]

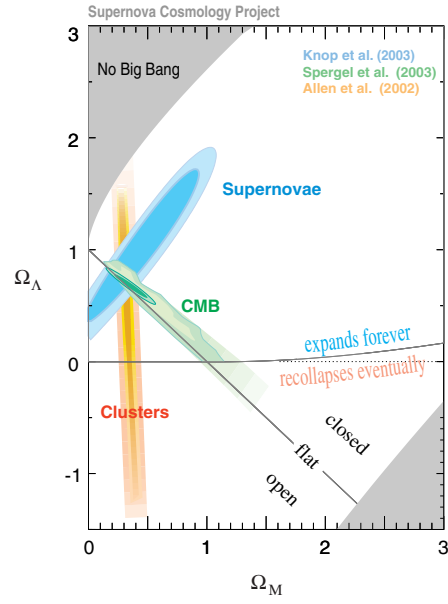


Figure 15. probability contours for  $\Omega_M, \Omega_\Lambda$  from CMB [16], galaxy clusters [17], SNIae [18]